SLAC–PUB–6062
March 1993
(A)

Fundamental–Mode rf Design in e^+e^- Storage Ring Factories*

P. B. Wilson

Stanford Linear Accelerator Center
Stanford University, Stanford, California 94309

1. Introduction

The difficulties arising in the design of the rf system for a factory-type storage ring lie mainly in two areas. First, a gap in the circulating beam current (on the order of 5% of the ring circumference) is required for ion clearing. Because of the high beam loading current, this gap produces a strong transient variation in the rf cavity voltage, which can in turn lead to a significant shift in the synchronous phases between bunches on either side of the gap. This phase shift would produce an unacceptable shift in the collision point, unless compensated by a corresponding shift in the bunch phases in the other ring. In order to work out the details of this compensation, the transient beams loading effects produced by the gap must be calculated quite carefully. A major goal of this chapter is to provide the insight and the basic analytic tools necessary for this analysis.

The second major problem for the fundamental mode rf design is also a consequence of the high average current (and the consequent large number of bunches) needed for a storage ring particle factory: longitudinal multibunch beam instabilities at sideband frequencies within the passband of the accelerating mode. These instabilities can be damped by an appropriate feedback system, as discussed elsewhere in these proceedings.[1] However, as background for this problem, we need to understand the phase and amplitude variations produced in the cavity voltage when the bunches undergo small-amplitude synchrotron oscillations. In the final section, the cavity voltage variation induced by such oscillations is calculated and applied to compute the Robinson damping time.

The emphasis throughout this chapter will be to provide a thorough understanding of beam loading effects. To this end, we begin in the next section with a calculation of the voltage induced in a cavity by a single point charge passing through it. The result will be a Green's function for beam loading problems. Once the solution for a point charge is known, the beam-induced voltage for a bunch with arbitrary longitudinal charge density profile, or for a train of such bunches, can then be constructed by an appropriate superposition.

*Work supported by Department of Energy contract DE–AC03–76SF00515.

Invited talk presented at the Joint US–CERN School on Particle Accelerators, Benalmadena, Spain, October 29–November 4, 1992.

2. Beam Loading by a Single Bunch

The derivation in this section relies on three basic assumptions. First, conservation of energy applies to the interaction between a moving charged particle and the fields in a cavity or accelerating structure. Second, we assume that superposition applies; that is, the net cavity field can be constructed as a vector (phasor) sum of component fields. Usually, this phasor is viewed in a reference frame rotating at either the cavity resonant frequency, or if there is an external generator driving the cavity, at the rf drive frequency. The third basic assumption is that the cavity fields are those for a single nondegenerate cavity mode which is orthogonal to all other modes. Thus a charge passing through a cavity independently deposits energy in each mode with which it can interact. We assume the conductivity of the cavity walls is sufficiently high so there is no significant coupling (overlap in impedance) with any other mode. We consider only the case of highly relativistic charged particles moving close to the speed of light. This has two consequences. First, the particle cannot change its velocity in response to beam-induced or generator-produced cavity fields. This allows a train of such particles to be modelled as a current generator in an equivalent circuit analysis of a beam-loaded cavity. Second, the cavity fields, summed over all cavity modes, must obey causality; that is, there is no net induced field ahead of a relativistic particle. This point will deserve further comment.

2.1 The Voltage and Energy Induced in a Cavity by a Point Charge

Assume that a charged particle moves through a cavity along the z-axis. In a given mode, the field at any point $E_z(z)$ is related to the energy U stored in the mode by

$$E_z(z) \;=\; \alpha(z)\, U^{1/2} \;. \tag{2.1.1}$$

A change in mode energy dU will produce a field change

$$dE_z(z) \;=\; \frac{\alpha^2(z)}{2E_z}\, dU \;.$$

On the other hand, a charge q moving through distance dz will lose energy

$$dU_q \;=\; -qE_z d_z \;.$$

This energy must go into energy stored in the cavity fields. The fields in this particular mode must then increase everywhere in the cavity during time $dt = dz/c$, even ahead of a particle moving at $v \approx c$. Causality does not apply to the cavity fields for a single mode, but it must of course be satisfied by a superposition of all modes. This is insured by the structure of Maxwell's equations, together with the cavity boundary conditions. By conservation of energy, dU (mode) $= dU_q$ (lost by charge), giving

$$dE_z(z) \;=\; -\frac{1}{2}\, q\alpha^2(z)\, dz \;. \tag{2.1.2}$$

This is the differential element of field induced by a charge in moving distance dz in the cavity. The minus sign indicates that the induced field opposes the motion of the charge. To calculate the net induced field, we must integrate the motion of the charge across the cavity, taking account of the fact that earlier induced differential field elements are rotating in phasor space according to $e^{j\omega_0 t}$, where ω_0 is the resonant frequency of the cavity. Calculating the net induced field at any time as the charge crosses the cavity is then a matter of adding up all of the field elements induced at earlier times. For convenience we choose a reference position $z = 0$ at the entrance

to the cavity, where $E_z(0) \equiv E_0$ and $\alpha(0) \equiv \alpha_0$. Then, assuming the position of the charge is given by $z = ct$, the change in field at the reference position during time dt is

$$dE_0(t) \;=\; [\alpha_0/\alpha(z)]\, dE_z(z) \;=\; -\frac{1}{2}\, qc\,[\alpha_0 \alpha(ct)]\; dt\;.$$

Using complex (phasor) notation, where a phasor quantity is denoted by a tilde, a field element induced at t' will ring as a function of time according to

$$\widetilde{dE}_0(t) \;=\; dE_0(t')\; e^{j\omega_0(t-t')}\;. \tag{2.1.3}$$

The net field at $z = 0$ at the time the charge exits from the cavity at $z = L$ and $t = L/c$ is then obtained as the superposition of all the differential field elements induced at earlier times, taking into account their proper phases:

$$\widetilde{E}_{0b}\,(t \;=\; L/c) \;=\; -\frac{1}{2} q\alpha_0 \int_0^L \alpha(z')\; e^{jk_0(L-z')}\; dz'\;, \tag{2.1.4}$$

where $k_0 = \omega_0/c$ and the subscript b indicates the beam-induced value. Note that $\widetilde{E}_{0b}$ is proportional to the charge times a factor that depends only on the geometry of the cavity mode, and not on the field amplitude. It will be useful to define a quantity k_ℓ, called the loss parameter for reasons which will become apparent, which depends on the mode configuration:

$$k_\ell \;\equiv\; \frac{\widetilde{V}\cdot\widetilde{V}^*}{4U} \;=\; \frac{V^2}{4U}\;. \tag{2.1.5}$$

Here $\widetilde{V}$ is the cavity voltage (and $\widetilde{V}^*$ the complex conjugate) seen by a test charge moving across the cavity according to $z = c(t - t_0)$ with $E_z(z,t) = E_z(z)\, e^{j\omega_0 t}$. The voltage seen in a frame of reference traveling with the particle is then

$$\begin{aligned}
&\widetilde{V} \;\equiv\; e^{j\omega_0 t_0} \int_0^L E_z(z')\; e^{jk_0 z'}\, dz' \;=\; V e^{j\omega t_0 + \theta}\;; \\
&V \;\equiv\; \left|\widetilde{V}\right| = \left(C^2 + S^2\right)^{1/2}\;; \qquad \tan\theta = S/C\;; \\
&C \;=\; \int_0^L E_z(z)\, \cos k_0 z\; dz\;; \qquad S \;=\; \int_0^L E_z(z) \sin k_0 z\; dz\;.
\end{aligned} \tag{2.1.6}$$

It is often convenient to define a reference plane at $z_r \equiv \theta/k_0$, such that the voltage gain of a test charge (electron) is given by $\widetilde{V} = V\, e^{j\omega_0 t_r}$, where t_r is the time at which the charge crosses the reference plane. Using the above definitions, together with Eq. (2.1.1) in Eq. (2.1.4) to eliminate $\alpha(z)$ and α_0, the beam-induced voltage becomes

$$\widetilde{V}_b \;=\; -2k_\ell q \left[e^{jk_0 L}\widetilde{V}^*/V\right]\;, \qquad V_b \;=\; \left|\widetilde{V}_b\right| \;=\; 2k_\ell q\;. \tag{2.1.7}$$

The quantity in brackets gives the phase of the beam-induced voltage with respect to the voltage defined by Eq. (2.1.6).

The voltage induced by a charge, as given by Eq. (2.1.7), is independent of any prior voltage present in the cavity. This is true because in equating dU (mode) to dU_q (lost by the charge) to obtain the differential beam-induced field element given by Eq. (2.1.2), both sides were proportional to the pre-existing field E_z, which therefore drops out of the final expression. The stored energy remaining in the cavity after the exit of the inducing charge must in general be calculated by first taking the vector (phasor) sum of the beam-induced voltage and any pre-existing voltage, and then

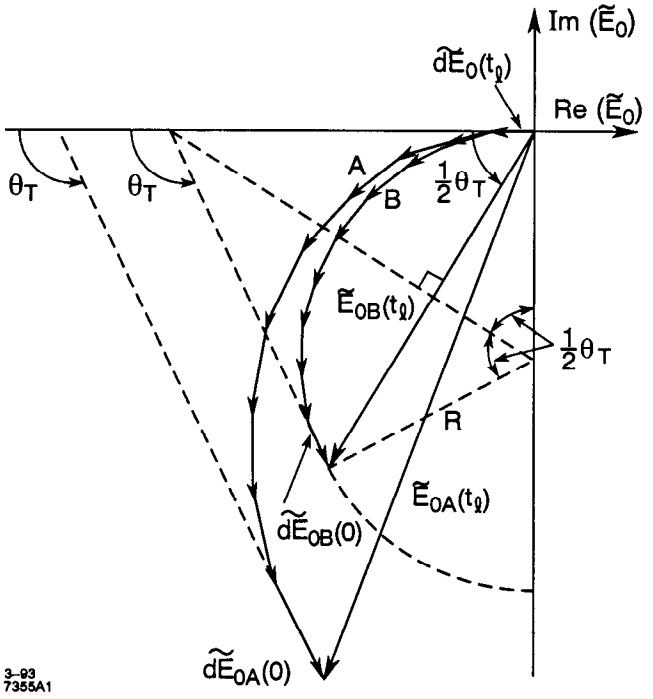

Figure 2.2.1. Differential superposition for two cases: (A) a mode in which E_z decreases along the particle trajectory; (B) a mode with constant E_z along the particle trajectory. In both cases, the field (for given stored energy) is assumed to be the same at $z = L$.

calculating the energy using Eq. (2.1.5). If there is no pre-existing cavity excitation, then the beam induced energy is given by combining Eqs. (2.1.5) and (2.1.7) to obtain

$$U_b = \frac{V_b^2}{4k_\ell} = k_\ell q^2 ; \tag{2.1.8}$$

hence the name *loss parameter* for the quantity k_ℓ. The effective voltage V_q "seen" by the charge is the voltage necessary to extract energy U_b, or

$$V_q = U_b/q = k_\ell q . \tag{2.1.9}$$

This is just one-half of the induced voltage left behind in the cavity. This result is sometimes called the Fundamental Theorem of Beam Loading. Crudely stated, the charge does not experience any retarding voltage as it starts to cross the cavity, while it sees the full induced voltage as it leaves the cavity. On the average, it might then be expected to see one-half of the final induced voltage.

2.2 Differential Superposition

Figure 2.2.1 shows the geometry of the superposition of the beam induced differential field elements for two cases. Case A shows an example in which the field function $\alpha(z)$ in Eq. (2.1.1) decreases with z, while case B is for a mode with a uniform electric field along the particle trajectory. The induced field elements are shown at time $t_\ell = L/C$, just as the particle leaves the cavity. Therefore the last induced field element lies

along the negative real axis of the phasor diagram. Following Eq. (2.1.3), an earlier field element induced at time $t = t'$ will have rotated in phasor space by an angle $\omega_0(t_\ell - t')$. The first field element induced at $t' = 0$ will have rotated by an angle (the transit angle) $\theta_T = \omega_0 L/c$. For the case of constant E_z, it is seen that the reduction in the induced field due to the fact that the particle takes a finite time to cross the cavity, as compared to the induced field for a charge of infinite velocity, is just the ratio of the chord length to the arc length shown in the diagram:

$$T = \frac{E_{oB}}{R\theta_T} = \frac{2R\,\sin(\theta_T/2)}{R\theta_T} = \frac{\sin(\theta_T/2)}{\theta_T/2} ,$$

where T is just the usual transit angle factor. The phase of the net beam-induced field is seen to be rotated by an angle $\theta_T/2$ with respect to the final induced element. This is also the phase of the field induced at the center (symmetry plane) of the cavity.

2.3 Bunch Form Factor

The voltage induced by an arbitrary charge distribution can be related to the charge induced by a point charge using a bunch form factor. The voltage at time t induced at time t' by a charge element $dq = I(t')dt'$ is

$$\widetilde{dV}(t) = -2k_\ell\, I(t')\, e^{j\omega(t-t')}\, dt' .$$

The total voltage induced by the charge distribution can be set equal to that induced by a point charge, reduced by a factor F_b and located at time t_0 (or at phase $\omega t_0 = \phi$),

$$\widetilde{V}(t) = -2k_\ell \int_{-\infty}^{\infty} I(t')\, e^{j\omega(t-t')}\, dt' = -2q\, k_\ell\, F_b\, e^{j(\omega t-\phi)} .$$

Solving for F_b and ϕ,

$$F_b = \left(C_S^2 + C_A^2\right)^{1/2} ; \qquad \tan\phi = \frac{C_A}{C_S} , \tag{2.3.1}$$

where C_S and C_A are the symmetric and antisymmetric integrals

$$C_S = \frac{1}{q}\int_{-\infty}^{\infty} I(t')\cos\omega t'\, dt' ; \qquad C_A = \frac{1}{q}\int_{-\infty}^{\infty} I(t')\sin\omega t'\, dt' .$$

If a charge distribution having a time-width which is not negligible compared to the rf period is accelerated across a cavity, the average energy gain per electron in the bunch is reduced by the same form factor. If $V_0\, e^{j\omega t}$ is the energy gain by a point particle crossing the cavity, then the charge-weighted average energy gain is

$$\widetilde{V}_{\rm ave} = \frac{V_0}{q}\int_{-\infty}^{\infty} I(t')\, e^{j\omega(t-t')}\, dt' = V_0 F_b\, e^{j(\omega t-\phi)} , \tag{2.3.2}$$

where F_b and ϕ are again given by Eq. (2.3.1). It is important to note that, for any charge distribution, both the average accelerating voltage and the net beam-induced voltage are reduced by exactly the same factor with respect to a point charge. The position (phase) of an effective point charge which replaces the distribution is also the same.

Some useful bunch form factors are:

$$F_b(\text{Gaussian}) = e^{-\omega_0^2\sigma_t^2/2} ,$$

$$F_b(\text{rectangular}) = \frac{\sin(\omega_0 T_b/2)}{\omega_0 T_b/2} ,$$

where σ_t is the rms bunch length (Gaussian) and T_b is the full bunch width (rectangular).

2.4 Summary Comments on Single Bunch Beam Loading

In this section we have tried to give a reasonably thorough understanding of the physics underlying the voltage induced in a cavity by a single bunch. If we add the fact that this voltage will decay as a function of time according to e^{-t/T_F}, where $T_F = 2Q_L/\omega_0$ is the loaded cavity filling time, then we have a Green's function for calculating any beam loading problem. The voltage induced by a train of bunches with arbitrary charges and spacing is then calculated by superposition. In the general case, of course, the voltage produced by an external generator must be included by a further superposition. In a storage ring, a strong constraint is added by the fact that, after initial damping, the bunches adjust their phases with respect to the net cavity voltage in a way such that each of the bunches gains the same energy (to make up for synchrotron radiation and impedance losses). This can add considerable complexity to beam loading calculations when bunch charges or bucket spacings are not equal—for example, when there is a gap in the circulating beam.

3. Beam Loading by a Train of Equally Spaced Bunches

3.1. Beam-Induced Voltage for Small Bunch Spacing

Using the definition of cavity voltage in Eq. (2.1.6), we can now define a cavity shunt impedance R in terms of the power P_c dissipated in the cavity walls, $R \equiv V^2/2P_c$. We assume the usual definitions for the Q's of the unloaded cavity, $Q \equiv \omega_0 U/P_c$, and loaded cavity, $Q_L \equiv Q/(1+\beta)$. Here $\beta \equiv P_e/P_c$ is the usual coupling coefficient for a coupling aperture or loop, such that P_e is the power emitted from the aperture into a matched load when there is no incoming rf wave from an external source. Taking the bunch spacing as ΔT_b, we have the following relations and definitions:

$$k_\ell \equiv \frac{V^2}{4U} = \frac{\omega_0}{2}\left(\frac{R}{Q}\right); \qquad \frac{R}{Q} = \frac{V^2}{2\omega_0 U}; \qquad \tau \equiv \frac{\Delta T_b}{T_f};$$

$$T_f = \frac{2Q_L}{\omega_0} = \frac{2Q}{\omega_0(1+\beta)}; \qquad V_{b0} = 2k_\ell q = \omega_0\left(\frac{R}{Q}\right) I_0 \Delta T_b = \frac{2I_0 R}{1+\beta}\cdot\tau\ , \tag{3.1.1}$$

where $I_0 = q/\Delta T_b$ is the dc current assuming equal bunch spacing. For a bunch current distribution of non-negligible time width, both V and V_{b0} must be reduced by the bunch form factor, as discussed in Sec. 2.3. A time reference is chosen such that the voltage V_{b0} induced by each of the bunches (assumed to be equally spaced) passing through the cavity lies along the negative real axis, following the convention in Sec. 2.3. We now assume that the bunch spacing is related to an rf frequency ω, which may be different from the cavity resonant frequency ω_0, such that $\omega\Delta T_b = 2\pi b$, where b is an integer (the number of rf wavelengths between bunches). Between successive bunches, the induced cavity voltage slips in phase (relative to a phasor coordinate frame rotating as $e^{j\omega t}$) by an amount

$$\delta = (\omega_0 - \omega)\,\Delta T_b$$

and decays in length by a factor $e^{-\tau}$. The process of the build-up of the net beam induced voltage is illustrated in Fig. 3.1.1, shown after a large number of bunches

have passed through the cavity. The net induced voltages just before and just after the bunch arrival time are denoted by $\widetilde{V}_b^-$ and V_b^+ where

$$\widetilde{V}_b^+ \;=\; -V_{b0}\left(1+e^{-\tau}\,e^{j\delta}e+e^{-2\tau}\,e^{2j\delta}+\ldots\right) \;=\; \frac{-V_{b0}}{1-e^{-\tau}\,e^{j\delta}}\;. \qquad (3.1.2)$$

Taking the limit $\Delta T_b/T_F \to 0$, such that $\tau, \delta \ll 1$,

$$\psi^+, \psi_a, \psi^- \;\longrightarrow\; \psi$$

$$\widetilde{V}_b^+, \widetilde{V}_{ba}, \widetilde{V}_b^- \equiv \widetilde{V}_b \;\longrightarrow\; -V_{b0}\cdot\frac{\tau+j\delta}{\tau^2+\delta^2} = -\frac{2I_0R}{1+\beta}\;\cos\psi e^{j\psi}$$

$$\tan\psi \;=\; \frac{\delta}{\tau} \;=\; (\omega_0-\omega)\,T_f = \frac{2Q_L}{\omega_0}(\omega_0-\omega)\;.$$

We see that ψ is just the usual *tuning angle*, which gives the variation in the phase of the beam-induced cavity voltage as the cavity is tuned off resonance. The magnitude of the induced voltage varies as $\cos\psi$, and therefore the tip of the phasor representing $\widetilde{V}_b$ follows a circle with diameter $2I_0R/(1+\beta)$ in phasor space as ψ is varied, as shown in Fig. 3.1.2. As is customary in complex notation, positive ψ is defined in the counter-clockwise direction.

If the series in Eq. (3.1.2) is summed to the n^{th} term,

$$\widetilde{V}_b^+(n) \;=\; -\frac{V_{b0}\left(1-e^{-n\tau}\,e^{jn\delta}\right)}{1-e^{-\tau}\,e^{j\delta}}\;.$$

Again let $\delta, \tau \to 0$ and approximate n by $t/\Delta T_b = t/\tau T_f$. The above expression then becomes

$$\widetilde{V}_b(t) \;=\; -\frac{2I_0R}{1+\beta}\;\cos\psi\;e^{j\psi}\left[1-e^{-t/T_F(1-j\,\tan\psi)}\right]\;. \qquad (3.1.3)$$

It is easy to show that transient variation of $\widetilde{V}_b(t)$, represented by the quantity in brackets, follows a logarithmic or equi-angular spiral (for example, see Ref. 2, Sec. 7.1). This is illustrated in Fig. 3.1.2, where a difference vector $\widetilde{V}_d(t)$ has been defined which connects $\widetilde{V}_b(t)$ to $\widetilde{V}_b(\infty)$. The tangent to the transient path followed by $\widetilde{V}_b$ always makes angle ψ with respect to $-\widetilde{V}_d$, which shrinks in time as $V_d(0)e^{-t/T_F}$ and rotates at a constant angular rate given by $e^{j(t/T_F)\,\tan\psi} = e^{j(\omega_0-\omega)t}$.

3.2 Relation to a Parallel–Resonant Equivalent Circuit

The result in Eq. (3.13) has been derived from basic principles, such as conservation of energy and superposition, with no reference to an equivalent circuit. However, this result is exactly what would be expected for the voltage induced by a current generator with rf current $\widetilde{I}_b = -2I_0$ across a parallel resonant circuit with shunt resistance R, shunt capacitance $1/C = \omega_0(R/Q) = 4k_\ell$, shunt inductance $\omega_0^{-1}(R/Q)$, and shunt resistance R/β to represent loading by the coupling network and external transmission line (assumed to be matched looking toward the generator; see Ref. 2, Sec. 3.5). Summarizing the results in the previous section, we have in the steady-state limit for the beam-induced voltage,

$$\widetilde{V}_b \;=\; -V_{br}\,\cos\psi\;e^{j\psi}\;, \qquad V_{br} \;=\; rV_{b0} \;=\; \frac{I_bR}{1+\beta} \;=\; \frac{2I_0R}{1+\beta}\;, \qquad (3.2.1)$$

where V_{br} is the magnitude of $\widetilde{V}_b$ at cavity resonance.

A current generator I_g can now be added to represent an external rf source driving the cavity. The rf power of the source is then identified as the available power from

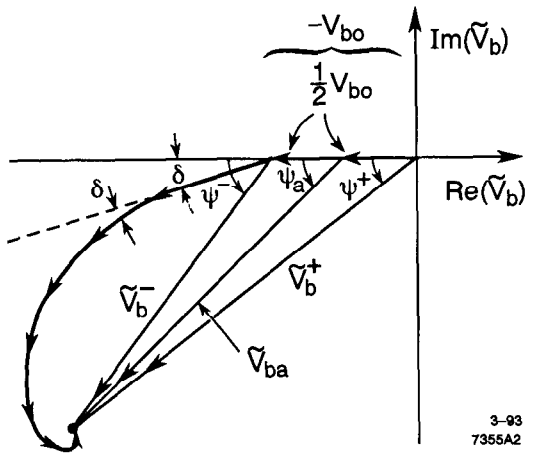

Figure 3.1.1. Diagram showing the buildup of the beam-induced voltage in a cavity by a train of equally-spaced bunches.

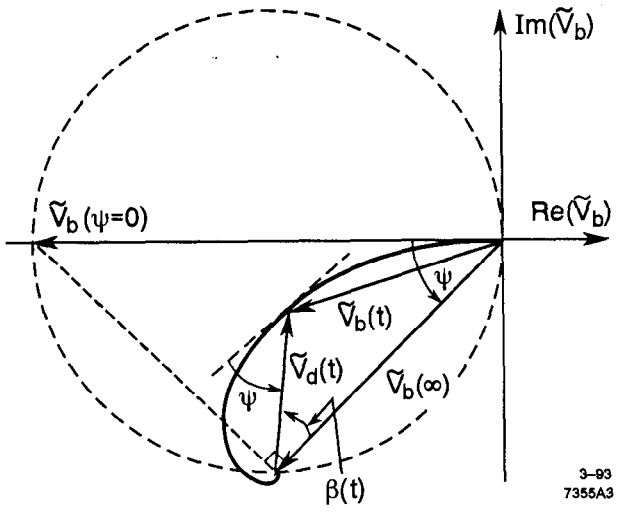

Figure 3.1.2. Diagram showing that the transient buildup of the beam-induced voltage $\tilde{V}_b(t)$, follows an equi-angular spiral (solid curve), where angle $\beta(t) = (\omega_0 - \omega)t = (t/T_F)\tan\psi$ and $V_d(t) = V_b(\infty)\ e^{-t/T_F}$. The steady-state beam-induced voltage, $\tilde{V}_b(\infty)$, follows a circle as cavity tuning is varied (dashed curve).

the generator, $P_g = I_g^2 R/8\beta$ (see, for example, the discussion in Ref. 2, Sec. 3.5). The voltage produced across the circuit is then

$$\widetilde{V}_g \;=\; V_{gr}\,\cos\psi\;\, e^{j\psi}\;, \qquad V_{gr} \;=\; \frac{I_g R}{1+\beta} = \frac{2\beta^{1/2}}{1+\beta}\cdot(2RP_g)^{1/2}\;\;. \tag{3.2.2}$$

Again note that if the bunch length is not small compared to the rf wavelength, both I_0 and I_g must be multiplied by the bunch form factor. From the form of Eq. (3.2.2), the tip of the phasor $\widetilde{V}_g$ also traces out a circle as the tuning angle ψ is varied, as shown for $\widetilde{V}_b$ in Fig. 3.1.2. If a step change is made in the driving generator voltage, $\widetilde{V}_g(t)$ also approaches a new steady-state value, $\widetilde{V}_g(\infty)$, along an equi-angular spiral. That is, the difference vector $\widetilde{V}_d(t) \equiv \widetilde{V}_g(t) - \widetilde{V}_g(\infty)$ shrinks in magnitude as e^{-t/T_F} and rotates in phase as $e^{j(\omega_0-\omega)t}$, in the same manner as $\widetilde{V}_d(t)$ in Fig. 3.1.2.

3.3 Bunch Spacing Comparable to the Cavity Filling Time

For a factory-type storage ring with a large number of bunches, the bunch spacing in time will be very small compared to the cavity filling time. There may, however, be occasion to calculate beam loading effects with only a few bunches in the ring (as is the case for most rings for high energy particle physics). The approximation $\tau \to 0$, and $\widetilde{V}_b^+ \approx \widetilde{V}_b^-$ cannot now be made. According to the Fundamental Theorem of Beam Loading, each bunch will experience the net voltage induced in the cavity by all bunches that have previously pass through it, $\widetilde{V}_b^-$, plus one-half of its own single-bunch induced voltage, $-\frac{1}{2}V_{b0}$. This is the voltage $\widetilde{V}_{ba}$ shown in Fig. 3.1.1. From Eq. (3.1.2),

$$\begin{aligned}\widetilde{V}_{ba} &= \widetilde{V}_b^- - \frac{1}{2}V_{b0} = \widetilde{V}_b^+ + \frac{1}{2}V_{b0} \\ &= -V_{b0}\left[\frac{1}{1-e^{-\tau}e^{j\delta}} - \frac{1}{2}\right] = -V_{b0}\,(F_R + jF_I)\;,\end{aligned} \tag{3.2.3}$$

$$\begin{aligned}F_R &= \frac{1-e^{-2\tau}}{2(1-2e^{-\tau}\,\cos\delta + e^{-2\tau})} \;\xrightarrow{\tau\to 0}\; \frac{\tau}{\tau^2+\delta^2} \\ F_I &= \frac{e^{-\tau}\,\sin\delta}{(1-2e^{-\tau}\,\cos\delta + e^{-2\tau})} \;\xrightarrow{\tau\to 0}\; \frac{\delta}{\tau^2+\delta^2}\;.\end{aligned}$$

The quantities F_R and F_I give the steady-state values of the real and imaginary parts of the beam-induced voltage after an infinite succession of charges have passed through the cavity, as compared with the voltage induced by a single passage of the charge. The quantity

$$2F_R = \Re e[\widetilde{V}_{ba}] \;\Big/\; -\frac{1}{2}V_{b0}$$

is sometimes called the resonance function, since it gives the net retarding voltage seen by a charge passing through a cavity with a resonant build-up of the beam-induced voltage, as compared to the voltage seen on a single passage. The resonance function is plotted and discussed in Ref. 2, Sec. 6.5.

In the limit of small τ, using $V_{b0} = \tau V_{br}$ and $\delta = \tau\tan\psi$, Eq. (3.2.3) approaches

$$\begin{aligned}\widetilde{V}_{ba} \;&\to\; -V_{br}\,[\tau F_R + j\tau F_I] \;=\; -V_{br}\,\cos\psi\, e^{j\psi} \\ \tau F_R \;&\to\; \cos^2\psi\;; \qquad \tau F_I \;\to\; \cos\psi\;\sin\psi\;.\end{aligned} \tag{3.2.4}$$

4. Steady–State Beam Loading in a Storage Ring RF System

4.1 Basic Phasor Diagram

In the previous sections the beam-induced voltage in a resonant cavity was derived from first principles, without an external rf generator. In this case, it is reasonable to choose a reference phase such that the beam-induced voltage at resonance lies along the negative real axis. We will follow this same conventions in drawing phasor diagrams for the general case in which an rf generator voltage component is present. This is at variance with the notation often used, which places the net cavity voltage along the positive real axis. There is not space here for a full discussion of the relative advantage and disadvantages of these alternative choices of a phasor reference frame. As a minimum, the reader will gain perspective by learning to view storage ring beam loading problems from a different vantage point.

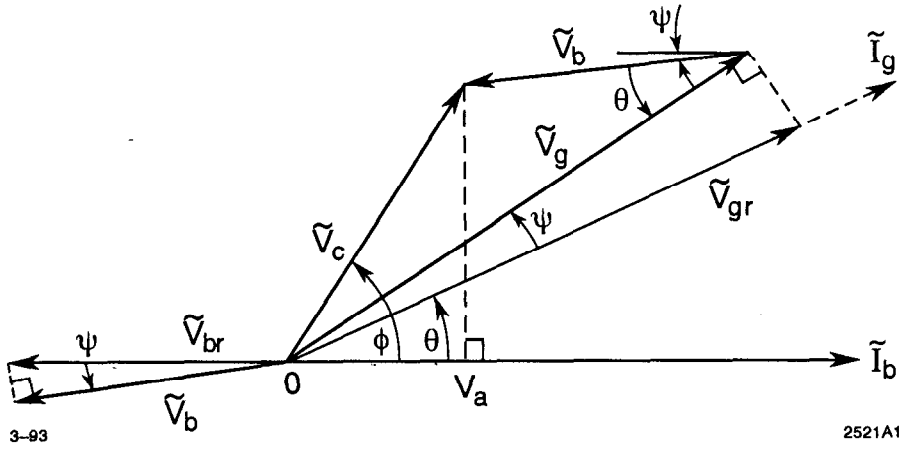

Figure 4.1.1. Diagram showing vector addition of generator and beam loading voltages in an RF cavity.

Figure 4.1.1 shows the basic phasor diagram in which the net cavity voltage, $\tilde{V}_c$, is obtained from the superposition of $\tilde{V}_g$ and $\tilde{V}_b$, as viewed in a reference frame rotating as $e^{j\omega t}$, where ω is the rf frequency and ω_0 the cavity resonant frequency. The beam current phasor lies along the positive real axis. The projection on this axis of the cavity voltage, lying at the synchronous phase angle ϕ, gives the accelerating component of the voltage. The generator current, which is colinear with the generator-induced voltage at resonance, $\tilde{V}_{gr}$, lies at an angle θ with respect to the real axis (and with respect to the beam current, I_b). As the cavity is tuned from resonance by a positive value of $\omega_0 - \omega$, both $\tilde{V}_g$ and $\tilde{V}_b$ rotate in the counter-clockwise direction through angle ψ, where $\tan\psi = 2Q_L(\omega_0 - \omega)/\omega$. It is also assumed that Q_L is relatively large .

From the diagram in Fig. 4.1.1, the real (accelerating) and imaginary components of the net cavity voltage $\tilde{V}_c$ are

$$\begin{aligned} V_A &= V_c \cos\phi = V_{gr} \cos\psi \cos(\theta+\psi) - V_{br} \cos^2\psi \,, \\ V_I &= V_c \sin\phi = V_{gr} \cos\psi \sin(\theta+\psi) - V_{br} \cos\psi \sin\psi \,. \end{aligned} \tag{4.1.1}$$

By eliminating $(\theta + \psi)$ from these two expressions (transfer the V_{br} components to the other sides of the equations, square, and add), then substituting for V_{gr} and V_{br}

using Eqs. (3.2.1) and (3.2.2), we obtain the required generator power in terms of V_c and ϕ for a given cavity tuning ψ and coupling β,

$$P_g = \frac{V_c^2}{2R} \cdot \frac{(1+\beta^2)}{4\beta} \cdot \frac{1}{\cos^2\psi} \left\{ \left[\cos\phi + \frac{2I_0R}{V_c(1+\beta)} \cos^2\psi \right]^2 + \left[\sin\phi + \frac{2I_0R}{V_c(1+\beta)} \cos\psi \sin\psi \right]^2 \right\} . \tag{4.1.2}$$

Angle θ is now fixed, and can be obtained, if desired, from either of Eqs. (4.1.1). In the general case when the bunch spacing is not small compared to the cavity filling time, the generator power can be obtained by substituting τF_R and τF_I for the factors $\cos^2\psi$ and $\cos\psi \sin\psi$ inside the brackets in Eq. (4.1.2), where F_R and F_I are given by Eq. (3.2.3); see Ref. 2, Sec. 6.4, for details.

4.2 Tuning Adjusted for Real Beam-Loaded Cavity Impedance

The reflected voltage from a beam-loaded cavity will look real (that is, it will have the same phase as the voltage reflected from the cavity at resonance without a beam) if the net cavity voltage $\tilde{V}_c$ is colinear with $\tilde{V}_{gr}$ (and therefore with $\tilde{I}_g$). From Fig. 4.1.1, this implies that $\theta = \phi$. Using this condition, and applying the law of sines to the phasor triangle in Fig. 4.1.1,

$$\frac{V_b}{V_c} = \frac{V_{br}\cos\psi}{V_c} = \frac{\sin(\phi-\theta-\psi)}{\sin\theta} = -\frac{\sin\psi_0}{\sin\phi} ; \qquad \tan\psi_0 = -\frac{V_{br}}{V_c}\sin\phi . \tag{4.2.1}$$

By differentiating Eq. (4.1.2) with respect to ψ, we find that $\psi = \psi_0$ is also the condition for minimum generator power (and hence minimum power reflected from the cavity). Substituting for ψ in Eq. (4.1.2) using the condition in Eq. (4.2.1), we have at optimum cavity tuning,

$$V_{gr0} = V_c + V_{br}\cos\phi , \qquad P_{g0} = \frac{(1+\beta)^2}{4\beta} \cdot \frac{V_{gr0}^2}{2R} . \tag{4.2.2}$$

By differentiating P_{g0} with respect to β, we find the value of cavity coupling which minimizes the generator power:

$$\beta_0 = 1 + \frac{2I_0R\cos\phi}{V_c} = 1 + \frac{P_b}{P_c} , \tag{4.2.3}$$

where $P_b = I_0V_c\cos\phi$. Using $P_g = P_b + P_c + P_r$, where P_r is the reflected power, it is easy to show that $P_r = 0$ if Eq. (4.2.3) is satisfied. If it is not, but if the cavity tuning is optimum according to Eq. (4.2.1), then the reflected power is

$$\frac{P_r}{P_c} = \frac{(\beta-\beta_0)^2}{4\beta} . \tag{4.2.4}$$

As a practical example, consider the PEP-II B-Factory rf system design with parameters[3] for the 9 GeV high energy ring (values are per cavity assuming 20 cavities):

$$V_c = 0.925 \text{ MV} , \quad I_0 = 1.5 \text{ A} , \quad \text{R} = 3.5 \text{ M}\Omega ,$$
$$V_A = V_s + I_0Z_{\text{hom}} \approx 0.192 \text{ MV} , \quad \phi = \cos^{-1} V_A/V_c = 78.0^\circ ,$$
$$P_c = V_c^2/2R = 122 \text{ kW} , \quad P_b = I_0V_A = 288 \text{ kW} .$$

Here $V_s = 0.18$ MV per cavity is the loss to synchrotron radiation, and $Z_{\text{hom}} \approx 9\ k\Omega$ allows for losses to higher modes in the rf cavity and to the real part of the per cavity

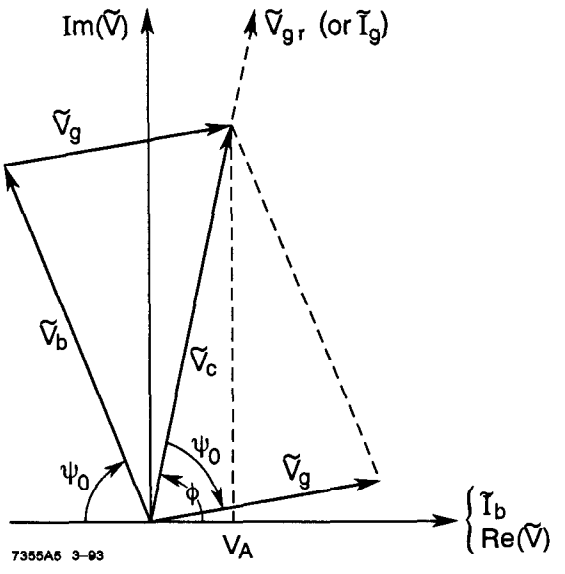

Figure 4.2.1. Phasor relationships for voltages in a PEP-II RF cavity at optimum tuning ($\tilde{I}_g$ colinear with $\tilde{V}_c$) and coupling (no reflected power).

share of the impedance of all other vacuum chamber components. The circulating current I_0 is set by the luminosity requirement, while the cavity voltage is set by bunch length and beam stability requirements, consistent with a reasonable klystron power. At optimum tuning and coupling, using (in order) Eqs. (4.2.3), (3.2.1), (4.2.2), and (4.2.1),

$$\beta_0 = 3.36\,, \quad V_{br} = 2.41 \text{ MV}\,, \quad V_{gr} = 1.425 \text{ MV}\,, \quad P_g = 410 \text{ kW}\,,$$

$$\psi_0 = -68.6^\circ\,, \quad V_b = V_{br}\cos\psi_0 = 0.88 \text{ MV}\,, \quad V_g = V_{gr}\cos\psi_0 = 0.52 \text{ MV}\,.$$

As a consistency check, note that the calculated generator power is just equal to the sum of the cavity wall losses and the power transferred to the beam, indicating that there is no reflected power at optimum coupling and tuning. In practice, the cavity coupling is often adjusted to be slightly greater than that given by Eq. (4.2.3), in order to make the rf system somewhat less sensitive to beam loading effects. For example, the cavity coupling might be set at $\beta = 4.0$ in the preceding example, rather than at 3.36. From Eq. (4.2.4), this increases the required generator power by 0.8% or 3 kW (the amount of the reflected power), but reduces V_{br} by 13% to 2.10 MV.

The phasor relationships in the example given above are plotted in Fig. 4.2.1. Note that if a klystron fails, the power dissipation in the cavity walls falls to $(0.88/0.925)^2 \times 122$ kW = 110 kW, while a reverse power $\beta P_c = 370$ kW is emitted from the cavity. If the beam should dump, but the klystron remain on, the power dissipated in the cavity is $(0.52/0.925)^2 \times 122$ kW = 40 kW, with a reflected power that is also equal to 370 kW. It is not a coincidence that this is exactly equal to the reverse power for the case of klystron failure. At optimum tuning and coupling, the wave emitted through the coupling aperture (or loop) by the beam-induced voltage component must exactly cancel the reflected wave due to the generator voltage component.

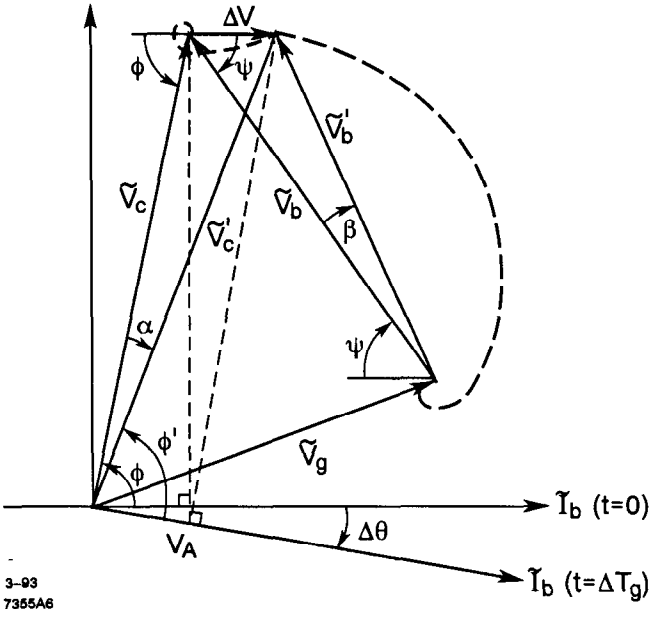

Figure 5.1.1. Phasor geometry for the case of a beam with a gap where $\tau_g \ll 1, \tau_b \gg 1$.

5. Beam Loading by a Circulating Beam with a Gap

5.1 Revolution Time T_0 Large Compared to the Cavity Filling Time

We first assume that the gap time, ΔT_g, is small compared to the cavity filling time, T_F, such that $\tau_g \equiv \Delta T_g / T_f \ll 1$. The basic assumption in this section is that the beam time, $T_b = T_0 - \Delta T_g$, is large compared to the cavity filling time such that $\tau_b \equiv T_b / T_F \gg 1$. This insures that the beam-induced voltage recovers very closely to its steady-state value after the passage of the gap. If this assumption is not met, the problem becomes considerably more complex and will be treated in Sec. 5.2. We will, however, be able to treat the more general case $\tau_g \approx 1$ later in this section, as long as the restriction $\tau_b \gg 1$ is kept.

The phasor geometry for the case $\tau_g \ll 1, \tau_b \gg 1$ is shown in Fig. 5.1.1. Here $\tilde{V}_b$ and $\tilde{V}_c$ are the steady-state values of the beam-loading and cavity voltages before the arrival of the gap, assumed to occur at time $t = 0$. A simple way to compute the voltage change ΔV is to assume that the actual ring current is continuous, but that a current of opposite sign, $-I_0$, is turned on at $t = 0$ for a time ΔT_g. The beam-induced voltage then must be along the positive real axis, as shown in Fig. 5.1.1, with a magnitude given by

$$\begin{aligned} \Delta V &= 2k_\ell q = \omega(R/Q) I_0' \Delta T_g = V_{br} \tau_g \\ I_0' &= I_0 \left[T_0 / (T_0 - \Delta T_g) \right] \approx I_0 \left(1 + \Delta T_g / T_0 \right) . \end{aligned} \tag{5.1.1}$$

As before, V_{br} and ΔV must be reduced by the bunch form factor, F_b in Eq. (2.3.1), in the case of long bunches. The magnitude of ΔV can be calculated in a second way, since we know that it is the beginning of the logarithmic spiral, shown by the dashed

line in Fig. 5.1.1, which eventually would end at the tip of the phasor $\widetilde{V}_g$ if the beam were not turned back on. Thus, according to the discussion following Eq. (3.1.3),

$$\widetilde{V}_b' = \widetilde{V}_b\, e^{-\tau_g} e^{j(\omega_0-\omega)t}\ , \qquad V_b' = V_b\, e^{-\tau_g} \approx V_b(1-\tau_g)\ ; \tag{5.1.2a}$$

$$\beta = (\omega_0-\omega)\,\Delta T_g = \tau_g \tan\psi\ . \tag{5.1.2b}$$

Applying the law of cosines to the triangle $\Delta V, \widetilde{V}_b, \widetilde{V}_b'$:

$$\Delta V = V_b\left[\left(1+e^{-2\tau_g}\right) - 2e^{-\tau_g}\,\cos\left(\tau_g\,\tan\psi\right)\right]^{1/2}\ . \tag{5.1.3}$$

Expanding assuming small τ_g, this reduces to $\Delta V \approx V_{br}\tau_g$, in agreement with Eq. (5.1.1). Now apply the law of cosines to compute V_c' in the phasor triangle $\Delta V, \widetilde{V}_c, \widetilde{V}_c'$ in Fig. 5.1.1:

$$V_c' = \left[V_c^2 + (\Delta V)^2 + 2V_c\Delta V\,\cos\phi\right]^{1/2} \tag{5.1.4a}$$

$$\approx V_c\left[1+(\Delta V/V_c)\,\cos\phi\right]\ . \tag{5.1.4b}$$

The law of sines gives angle α in the same triangle:

$$\sin\alpha = \left(\Delta V/V_c'\right)\,\sin\phi\ , \tag{5.1.5a}$$

$$\alpha \approx (\Delta V/V_c)\,\sin\phi\ . \tag{5.1.5b}$$

The shift in beam phase across the gap, measured in a reference frame provided by the external rf generator (see Fig. 5.1.1), is

$$\Delta\theta = \alpha + \left(\phi'-\phi\right)\ , \tag{5.1.6}$$

where, using Eq. (5.1.4b),

$$\cos\phi' = V_A/V_c' \approx \cos\phi\left[1-(\Delta V/V_c)\,\cos\phi\right]\ . \tag{5.1.7}$$

Using the trigonometric expression for $[\cos\phi' - \cos\phi]$ to expand Eq. (5.1.7), the shift in bunch phase given by Eq. (5.1.6) is

$$\Delta\theta \approx \frac{\Delta V}{V_c}\,\sin\phi + \left[\left(\tan^2\phi + 2\frac{\Delta V}{V_c}\,\cos\phi\right)^{1/2} - \tan\phi\right]\ , \tag{5.1.8}$$

where the term in brackets is the change in synchronous phase, $\phi'-\phi$. For ϕ near 90°, $\phi' \approx \phi$ and $\Delta\phi \approx \alpha \approx \Delta V/V_c$. For ϕ near zero, $\alpha \approx 0$ and $\Delta\phi \approx \phi'-\phi \approx (2\Delta V/V_c)^{1/2}$.

It is now easy to lift the restriction $\tau_g \ll 1$, although we will not be able to write an explicit expression for $\Delta\theta$. In Fig. 5.1.1, $\widetilde{\Delta V}$ is now a phasor which no longer lies in the positive real direction, but instead has its tip anywhere along the dashed spiral. Equation (5.1.3) can be used to find its magnitude. The angle between $\widetilde{\Delta V}$ and $\widetilde{V}_b$ will no longer be ψ, but something less, $\psi-\delta$ (see Fig. 5.1.2). This angle can be computed using the law of sines:

$$\sin\,(\psi-\delta) = \left(V_b'/\Delta V\right)\,\sin\beta = \left[V_b\,e^{-\tau_g}/\Delta V\right]\,\sin\left(\tau_g\,\tan\psi\right)\ .$$

Equation (5.1.4a) can now be used to compute V_c', replacing ϕ by $\phi+\delta$. Equation (5.15a) is then used to compute angle α, again replacing ϕ by $\phi+\delta$. Angle ϕ' is obtained as $\phi' = \cos^{-1}\left(V_A/V_c'\right)$.

As a numerical example, consider the case of the PEP-II B factory with a 5% gap in the circulating beam. For PEP-II, some relevant rf parameters are[3]: rf frequency, 476 MHz; $T_0 = 7.34\times10^{-6}$ sec; loss parameter $k_\ell = (\omega/2)(R/Q) \approx 1.74\times10^{11}V/C$; loaded cavity $Q, Q_L \approx 6,700$ for a cavity coupling coefficient of 3.5. Thus the filling time is $2Q_L/\omega \approx 4.5\times10^{-6}$ sec, and $\tau_g \approx 0.08, \tau_b \approx 1.6$. We see that the basic assumption of this section, $\tau_b >> 1$, is not very well met. If we proceed anyway to compute $\Delta\theta$, Eq. (5.1.3) gives $\Delta V \approx 0.19$ MV for a circulating current of 1.5A. For a synchronous phase angle of 78° and a cavity voltage of 0.925 MV, Eq. (5.1.8) gives $\Delta\theta = 12°$.

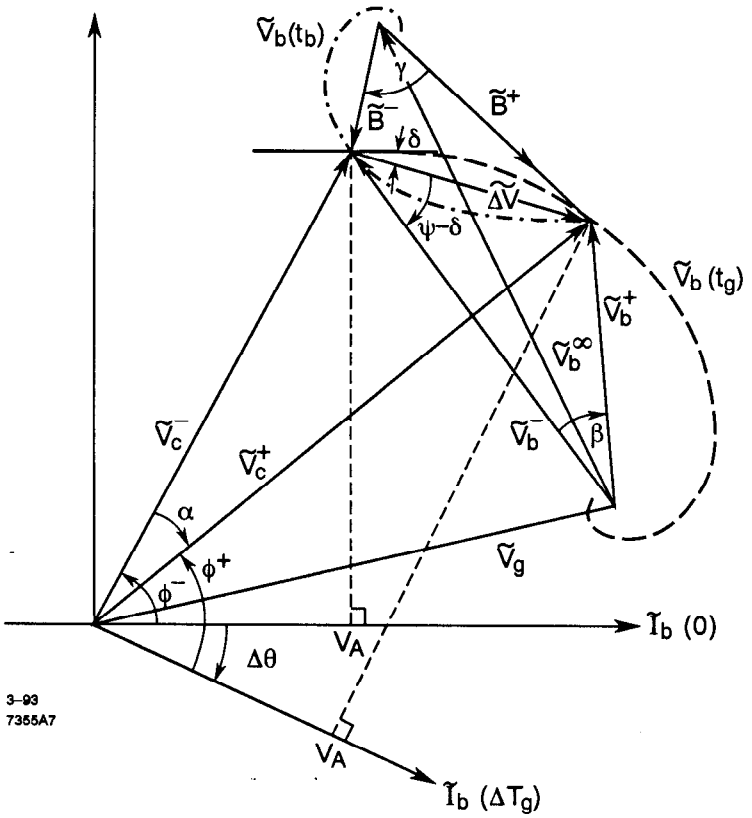

Figure 5.1.2. Phasor geometry for a beam with a gap with arbitrary τ_g and τ_b.

5.2. Gap with Arbitrary Values of τ_g and τ_b

Figure 5.1.2 shows the phasor geometry for the case of a beam gap where both the gap time and beam time are of arbitrary length with respect to the cavity filling time. The basic phasor reference frame is again chosen so that the phase of the last bunch before the gap begins, at time $t = 0$, lies along the positive real axis. During time $0 < t/T_f < \tau_g$ the beam-induced voltage component progresses along the logarithmic spiral $\tilde{V}_b(t_g)$, shown by the dashed curve, starting at $\tilde{V}_b^-$ at $t = 0$ and ending at $\tilde{V}_b^+$ at $t/T_f = \tau_g$. During time $\tau_g < t/T_F < \tau_g + \tau_b$, the phasor $\tilde{V}_b$ travels along the dot-dashed curve, driven by a current $I_0' = I_0\tau_0/\tau_b$, where $\tau_0 \equiv T_0/T_F = \tau_b + \tau_g$. At time $t = T_0$, the phasor is exactly back at $\tilde{V}_b^-$. If the current were to continue, instead of the gap arriving again at $t = T_0$, the tip of the phasor would continue along the dot-dashed curve $\tilde{V}_b(t_b)$ to the steady-state position, $\tilde{V}_b^\infty$.

The transient beam loading problem would be relatively simple if we were dealing with a standing-wave linac cavity, driven by an incoming beam with a periodic gap. From Fig. 7, we could in this case write the following phasor relation:

$$\tilde{V}_b^+ = \tilde{V}_b^- \, e^{-\tau_g} \, e^{j\beta} \equiv \tilde{T}_g \tilde{V}_b^- \ , \qquad (5.2.1)$$

where τ_g and $\beta = \tau_g \tan\psi$ are known. Similarly,

$$\widetilde{B}^- = \widetilde{B}^+ \, e^{-\tau_b} \, e^{j\gamma} \equiv \widetilde{T}_b \, \widetilde{B}^+ \ , \tag{5.2.2}$$

where τ_b and $\gamma = \tau_b \tan\psi$ are also known. We also have

$$\widetilde{V}_b^- = \widetilde{V}_b^\infty + \widetilde{B}^- = \widetilde{V}_b^\infty + \widetilde{T}_b \widetilde{B}^+ \ , \qquad \widetilde{V}_b^+ = \widetilde{V}_b^\infty + \widetilde{B}^+ = \widetilde{T}_g \widetilde{V}_b^- \ ,$$

where $\widetilde{V}_b^\infty$ is known from Eq. (3.2.1). Eliminating $\widetilde{B}^+$ from these two equation and solving for $\widetilde{V}_b^-$,

$$\widetilde{V}_b^- = \widetilde{V}_b^\infty \left[\frac{\widetilde{T}_b - 1}{\widetilde{T}_b \widetilde{T}_g - 1} \right] \equiv \widetilde{A} \widetilde{V}_b^\infty \ , \qquad \widetilde{V}_b^+ = \widetilde{T}_g \widetilde{V}_b^- = \widetilde{A} \widetilde{T}_g \widetilde{V}_b^\infty \ . \tag{5.2.3}$$

Expressions for the cavity voltage phasors before and after the gap can now be written in terms of known quantities as

$$\widetilde{V}_c^- = \widetilde{V}_g + \widetilde{V}_b^- = \widetilde{V}_g + \widetilde{A} \widetilde{V}_b^\infty \ , \qquad \widetilde{V}_c^+ = \widetilde{V}_g + \widetilde{V}_b^+ = \widetilde{V}_g + \widetilde{A} \widetilde{T}_g \widetilde{V}_b^\infty \ . \tag{5.2.4}$$

Since the timing of the bunches is set by an external generator (the injector) in the case of a linac, the bunch phase $\widetilde{T}_b$ stays constant. The bunches before and after the gap therefore see different accelerating voltages, given by the real parts of $\widetilde{V}_c^-$ and $\widetilde{V}_c^+$.

In the case of a storage ring with standing-wave cavities, the situation is more complex because the bunch phases will adjust themselves, on a time scale on the order of the damping time, to pick up a constant accelerating voltage (the synchronous energy gain). Thus the reference phase at the end of the gap must rotate through angle $\Delta\theta$, in Fig. 5.1.2. During the beam-on time, angle γ in Fig. 5.1.2 must change to take this into account:

$$\gamma = \tau_b \tan\psi - \Delta\theta \ . \tag{5.2.5}$$

Thus $\widetilde{T}_b$ in Eq. (5.2.2), $\widetilde{A}$ in Eqs. (5.2.3) and consequently both $\widetilde{V}_c^-$ and $\widetilde{V}_c^+$ in Eqs. (5.2.4) are functions of $\Delta\theta$. On the other hand, if $\widetilde{V}_c^-$ and $\widetilde{V}_c^+$ are given, the value of $\Delta\theta$ is readily calculated:

$$\begin{aligned} \Delta\theta &= \alpha + \phi^+ - \phi^- \ , \\ \phi^+ &= \cos^{-1}\left(V_A / V_c^+\right) \ , \qquad \phi^- = \cos^{-1}\left(V_A / V_c^-\right) \ , \\ \alpha &= \tan^{-1}\left[\Im m\left(\widetilde{V}_c^-\right) \Big/ \Re e\left(\widetilde{V}_c^-\right) \right] - \tan^{-1}\left[\Im m\left(\widetilde{V}_c^+\right) \Big/ \Re e\left(\widetilde{V}_c^+\right) \right] \ . \end{aligned} \tag{5.2.6}$$

Thus $\Delta\theta$ must be calculated by a self-consistent procedure: assume values for $\Delta\theta$ in Eq. (5.2.5), then carry through the preceding calculation for V_c^+ and V_c^- until the value for $\Delta\theta$ in Eq. (5.2.6) is in agreement with the initial assumed value.

We see, even in the simple case of a gap in a beam with bunches of equal charge, that just the calculation of the bunch phase shift across the gap has become quite complicated. If further information is desired, for example the phase positions of other bunches, or perhaps the effects due to unequal bunch charges, it would be difficult, or at least very awkward, to carry out the calculation analytically. It might then be best to resort to a simulation, in which the phase and energy of each bunch is tracked turn by turn. Such a program would show all the features of the longitudinal bunch dynamics, such as phase oscillations after injection, Robinson damping of these oscillations, and variations in the cavity voltage due to transient beam loading. A tracking program of this type has been written for the SLC damping ring to show transient effects at injection, and to determine the optimum injection phase and energy.[4]

5.3 Cures for the Gap-Induced Phase Shift

One obvious way to reduce the effect of a gap-induced phase shift on the longitudinal position of the collision point is to put a similar gap in the counter-rotating low-energy beam. However, the beam current, cavity voltage and synchronous phase angle are slightly different for the PEP-II low energy beam[3]: $I_0 = 2.15$A, $V_c = 0.95$MV, $\phi_s = 80.5°$, $P_b = 335$ kW. Using Eq. (4.2.3), the optimum cavity coupling coefficient is $\beta = 3.6$ for $P_c = 129$ kW, giving $\tau_g = .084$ for $Q_0 = 3.0 \times 10^4$. From Eq. (3.2.1), $V_{br} = 3.27$ MV and from Eq. (4.2.1) the optimum tuning angle is $-73.6°$. Then $V_b = V_{br}\cos\psi = 0.95$ MV, and Eq. (5.1.3) now gives $\Delta V = 0.26$ MV. Finally, Eq. (5.1.8) gives $\Delta\theta \approx 16°$. Since the high-energy beam has a phase shift of 12°, a residual phase shift of 4° remains. This is still large enough to produce a shift in the position of the collision point of 7 mm for $\lambda_{rf} = 63$ cm. This a substantial fraction of the bunch length, $\sigma_z = 10$ mm. This residual phase shift can be eliminated entirely if the current is reduced to 25% in the gap in the low-energy beam, instead of to zero.

Another possibility remains for reducing the residual phase shift across the beam gap. It is clear that if the rf generator voltage component $\widetilde{V}_g$ in Fig. 4.2.1 is jumped in phase and amplitude such that $\widetilde{\Delta V}_g = -\widetilde{V}_b$, then the transient effect of the gap is completely eliminated. However, this would require an increase in klystron power by a factor of $(V_c/V_g)^2 = (.925/.52)^2 = 3.2$, which is clearly not practical. However, we should calculate how much of a reduction in the gap phase shift can be obtained by a jump in klystron phase alone. Suppose the phase is shifted such that $\widetilde{V}_g' = \widetilde{V}_g e^{j\eta}$ at the beginning of the gap, where η is a counter-clockwise rotation of $\widetilde{V}_g$ in Fig. 5.1.1. We will not give all the details, but will only outline the calculation here. First a difference phasor $\widetilde{D}$ is defined such that $\widetilde{V}_g' + \widetilde{D} = \widetilde{V}_c$, where the angle between $\widetilde{V}_g'$ and $\widetilde{V}_c$ is $\eta - |\psi|$, where we assume $\widetilde{V}_c$ is colinear with $\widetilde{V}_{br}$. The law of cosines is used to calculate the magnitude of $\widetilde{D}$. During the gap period, the phasor $\widetilde{D}$ rotates through angle $\tau_g \tan\psi$ to position $\widetilde{D}'$, where $D' = De^{-\tau_g}$. The third side of this second phasor triangle is $\widetilde{\Delta V}$, which is calculated by the law of cosines. The angle opposite $\widetilde{D}'$, call it ψ', can now be computed by the law of sines. We will also need the angle opposite $\widetilde{V}_g'$ in the first phasor triangle, call it γ, where γ can also be computed using the sine law. Now establish a third phasor triangle, $\widetilde{V}_c, \widetilde{V}_c', \widetilde{\Delta V}$. The angle between $\widetilde{V}_c$ and $\widetilde{\Delta V}$, call it δ, is given by $\delta = \psi' - \gamma$. V_c' is now calculated by the cosine law, and angle α opposite $\widetilde{\Delta V}$ by the sine law. Angle ϕ' is now given by $\cos^{-1}(V_A/V_c')$, and the gap phase shift by $\Delta\theta = \alpha + \phi' - \phi$. Applying this procedure to the parameters of the PEP-II high energy ring, we calculate that the gap can be reduced to about 3° for $\eta \approx 100°$, with $\Delta V = 0.12$ MV and $V_c' = 0.83$ MV. This is a reduction by a factor of four from the 12° phase shift without the jump in generator phase. If a similar phase jump is carried out for the low energy beam, the residual phase error would be reduced from 4° to about 1°. This produces a collision point shift of about $0.2\sigma_z$, which may be acceptable.

Finally, feedback can also be used to reduce the transient effects due to the gap (see Ref. 1).

6. Phase Stability and Phase Oscillations

6.1 Phase Stability

In an electron storage ring it is well known that, to be stable against phase perturbations, a particle must have a synchronous phase on the time-falling part of the

rf wave. For example, a particle having too much energy compared to a synchronous particle will follow a longer path and will therefore receive less energy from the rf cavity on the next revolution. A particle that arrives at the rf cavity too early compared to a synchronous particle will get more than the synchronous energy gain, will consequently take a longer path and will arrive back at the cavity closer to the synchronous passage time. Using $V_A = V_c \cos[\omega(t - t_s) + \phi_s]$, the condition $dV_A/dt < 0$, evaluated at $t = t_s$, leads to $(-\omega V_c \sin\phi_s) < 0$, or $\sin\phi_s > 0$. Of course, ϕ_s must also be less than $\pi/2$ if V_A is to be positive. At high current, where the beam-induced voltage component is large, the situation is more complicated. As the arrival time varies due to phase oscillations, the beam-induced voltage component moves with the bunch and hence cannot contribute to phase stability; only the generator voltage component can provide a restoring force against phase perturbations. From Fig. 4.1.1 we see that the phase of the generator voltage component with respect to the beam is $\theta + \psi$, and hence the condition $dV_g/dt < 0$ at $t = t_s$ leads to $\sin(\theta + \psi) > 0$, or from Eq. (4.1.1),

$$2V_c \sin\phi + V_{br} \sin 2\psi > 0 \,. \tag{6.1.1}$$

This is the condition for the high-current limit on phase stability first derived by Robinson. Robinson's derivation involved setting up a set of linear equations in terms of slow (compared to the rf frequency) perturbations to the variables of the system. He then applied Routh's criterion to the determinant of the coefficients to test for exponentially growing solutions. However, the result is completely equivalent to the simple condition $dV_g/dt < 0$, which leads directly to Eq. (6.1.1) using the geometry of the basic phasor diagram in Fig. 4.1.1. If the cavity tuning is adjusted to make the beam-loaded cavity voltage look real, then Eq. (5.1.1), together with Eq. (4.2.1) gives

$$V_c > V_{br} \cos\phi \quad . \tag{6.1.2}$$

If the cavity coupling is also optimized according to Eq. (4.2.3), then $V_{br} \cos\phi = V_c(\beta_0 - 1)/(\beta_0 + 1)$ and the condition in Eq. (6.1.2) is always satisfied.

6.2 Phase Oscillations

There is not space here for a complete derivation from first principles of the damping time for phase oscillations. A derivation emphasizing the time-domain behavior of phasor quantities subject to small perturbations is given in Ref. 2, Sec. 4.2. A more traditional derivation is given in, for example, Ref. 5. The result for the growth rate (inverse of the damping time) of the oscillation is

$$\frac{1}{t_d} = \frac{V_{br}\,\omega_s}{V_c \sin\phi} \cdot \frac{\xi\eta}{[1 + (\xi + \eta)^2][1 + (\xi - \eta)^2]} \,, \tag{6.2.1}$$

where $\xi = \tan\psi = (\omega_0 - \omega)\,T_f$ and $\eta = \omega_s T_F$. The synchrotron oscillation frequency is given by

$$\omega_s = \left[\frac{\alpha_m\,\omega\,V_c \sin\phi}{T_0\,E_0}\right]^{1/2} \,, \tag{6.2.2}$$

where E_0 is the beam energy in volts and α_m is the momentum compaction factor. From Eq. (6.2.1) we see that the oscillations are damped if $\tan\psi$ is negative; that is, if the rf frequency is greater than the cavity resonant frequency. This is the case if ψ is optimized according to Eq. (4.2.1) to produce a real beam-loaded cavity reflection coefficient. The damping rate given by Eq. (6.2.1) vanishes if either ξ or η approaches zero or infinity. For small η, the function on the right-hand side of Eq. (6.2.1) has a maximum value of 0.32 η for $\xi = 0.58$ ($\psi = 30°$). For large η, the function has a maximum value of 0.25 for $\xi \approx \eta$. Equation (6.2.1) can also be used to calculate the growth or damping rate of the coupled-bunch longitudinal instability due to a higher mode in the rf cavity or to a resonance in another vacuum chamber component. In this case, the growth or damping rate given by Eq. (6.2.1) must be multiplied by the ratio of the mode frequency to the frequency of the accelerating mode.

The physical origin of this damping (Robinson damping) can be traced to the inertia of the stored energy in the rf cavities. Because of the finite filling time, the beam-induced voltage cannot follow changes in the beam current instantaneously. A phase difference between the induced voltage and the driving current oscillation appears, which in turn leads to an energy interchange between the oscillation and the cavity fields. A similar effect is seen in other physical systems, for example, the excitation of mechanical oscillations is the walls of a superconducting cavity.[6]

References

1. F. Pedersen, these proceedings.
2. P. B. Wilson, "High Energy Electron Linacs: Applications to Storage Ring RF Systems and Linear Colliders," in *Physics of High Energy Particle Accelerators*, AIP Conference Proceedings No. 87 (American Institute of Physics, New York, 1982), pp. 450–563; also SLAC–PUB–2884 (1982).
3. "An Asymmetric B Factory: Conceptual Design Report," LBL PUB–5303; also SLAC–372 (1991).
4. P. Wilson and T. Knight, Internal SLAC Notes CN–38, 43, 74 and 86 (1981).
5. A. Hofmann in *Theoretical Aspects of the Behavior of Beams in Accelerators and Storage Rings* (Proceedings of the First Course of the International School of Particle Accelerators, Erice, November 1976); CERN 77–13 (1977), p. 139.
6. P. H. Ceperly, IEEE Trans. Nucl. Sci. **NS–19**, No. **2**, 217 (1972).